

Photo-oxidative kinetics of solvent and oil-based terpenoid varnishes

Daniele Ciofini⁽¹⁾, Jana Striova⁽²⁾, Mara Camaiti⁽³⁾ Salvatore Siano⁽¹⁾

⁽¹⁾ *Istituto di Fisica Applicata “N. Carrara”, CNR, Via Madonna del Piano 10, 50019, Sesto Fiorentino, Italy.*

⁽²⁾ *Istituto Nazionale di Ottica, CNR, Largo Fermi 6, Firenze, Italy*

⁽³⁾ *Istituto di Geoscienze e Georisorse, CNR, Via G. La Pira 4, Florence, Italy*

Abstract

Here, the photo-oxidative degradation of several terpenoid varnishes usually encountered in conservation of cultural heritage has been investigated. Samples were prepared by dissolving dammar, mastic, colophony, sandarac and bleached shellac in suitable solvents or by heating mastic, colophony, sandarac and Manila copal with linseed oil. The alteration effects of this broad set of samples induced by light exposure in an ageing chamber, were thoroughly characterized using transmission FTIR spectroscopy, colorimetry, and gravimetric measurements. The various varnishes exhibited a similar saturating photo-oxidative kinetics upon the exposure time but significant quantitative differences were pointed out. A decreasing of the methyl and methylene stretching bands was observed for both solvent and oil based varnishes, which suggests the alteration effects begin with hydrogen atom abstractions. The consequent reaction with oxygen, catalyzed by irradiation and temperature rise lead to the increase of carbonyl and hydroxyl functionalities, thus suggesting the formation of new compounds containing carboxylic, ketone and ester groups and lactonised structures. At the same time, cross-linking and extensive polymerization were clearly observed for sandarac and shellac solvent varnishes. Measurement and comparison of the photo-oxidative and discoloration effects of the present set of samples, provide a general picture of the ageing phenomenology of the natural varnishes, which can be usefully exploited in characterization and conservation of easel paintings and other artworks.

INTRODUCTION

Natural varnishes have been applied on paintings and other art object since ancient times as protective coatings and in order to enhance both the color saturation and the overall gloss [1-4]. Resins mixed with a drying oil were the earliest type of varnish blend used in the Middle Ages, whereas the so called “spirit varnishes” (resin-solvent mixings) were marketed later in the sixteenth century. These have been widely used by the artists up until the World War II [4-5]. Afterwards, the introduction of synthetic products have drastically reduced the use of natural varnishes, although some of them are still in use.

Materials and preparation procedures have undergone a continuous evolution over the time, according to the different artistic and/or conservation-restoration needs. As regards the painting varnishes, numerous recipes are reported in historical treatises and artist' accounts [6-10]. The most relevant resins employed involve complex mixtures of terpenoid compounds, which can be grouped

according to their number of carbocyclic rings in sesquiterpenoids (compounds with 15 carbon atoms, such as shellac), diterpenoids (compounds with 20 carbon atoms, such as colophony, Venice turpentine, sandarac, copal) and triterpenoids (compounds with 30 carbon atoms, such as mastic, dammar, elemi) [3, 11]. Oil varnishes were usually prepared by mixing these resins with a drying oil such as poppy, nut and/or linseed oil, and heated at relatively high temperatures (300-350 °C).

Both spirit and oil varnishes can undergo different ageing processes over time: photo-, thermal and/or bio-degradation. Among these, the main recognized degradation pathway, which is of general valence for all the organic molecules, involves a well-known auto-oxidative process through chain radical reactions. This occurs both in light and darkness according to different kinetics, as shown for triterpenoid resin varnishes [12]. Radical chain reactions are usually initiated by absorption of UV light although the photon energies associated with short-wavelength visible light may cause photo-dissociation reactions as well [2,13,16]. These can also be driven by the thermal energy as well air pollutants and ozone [13-16]. Such radical reactions generate carbon structures with oxygen containing functional groups, which represent the beginning (primary reactions) of the autoxidation processes leading to radical polymerization (cross-linking or condensation), oxidative modifications, shortening of the side chain and probably defunctionalization, bond-breaking and disintegration of the terpenoid carbon skeleton [17].

As reported by various authors, the ageing effects under UV light exposure vary for each class of terpenoid compounds [15,17,18,19,20]. In particular, the major constituting resinous keto groups of mastic and dammar undergo bond homolysis and A-ring opening *via* Norrish type I reaction leading to highly oxidized and yellowed products [17, 20-21]. Copal and sandarac resins exhibit cross-linking and cleavage reactions, which lead to high molecular weight, crosslinked and saturated molecules consisting of bicyclic structures connected by a polymer chain [18]. Conversely, colophony shows dehydrogenation and aromatization reactions because of the high content of abietane acids with highly reactive C=C inside the rings. The ageing of shellac was interpreted as the result of a self-esterification process [22, 23], being this resin constituted mainly by several ester linkages. However, further insights are needed in order to completely characterize the photo-ageing behavior of the terpenoid varnishes. A few studies were reported on the diterpenoids, no data are available on bleached shellac and on the whole class of oil varnishes.

Here, the temporal evolution of the oxidation and polymerization pathways under artificial sunlight of a wide set of solvent and oil terpenoid varnishes have been investigated. Comparative quantitative evaluations of the photo-degradation kinetics of these two classes of products have been achieved using FTIR spectroscopy, colorimetry and gravimetric measurements. The results achieved provide a general picture of the ageing phenomenology of the terpenoid resin varnishes, and include original data on oil based varnishes and bleached shellac, which can be exploited in characterization and conservation treatments of easel paintings and other artworks.

EXPERIMENTAL

Sample preparation

Solvent and oil based varnishes were formulated according to the traditional recipes [6-10] using the products listed in Table 1, which are marketed by Zecchi, Florence.

Table 1 Prepared solvent and oil based varnishes. The concentration of cobalt in linseed oil, used as drier, was lower than 0.05 %.

Sample code	Resin	Binder	Solvent	wt
Dam-Spi	Dammar	-	white spirit,	30/70
Dam-Chl	Dammar	-	chloroform	30/70
Mast-Prop	Chios mastic	-	iso-propanol	30/70
Col-Eth	Colophony	-	ethanol	30/70
San-Eth	Sandarac standard	-	ethanol	30/70
She-Eth	Light shellac (bleached)	-	ethanol	30/70
Oil-Mast	Chios Mastic	Linseed oil	Rectified turpentine oil	30:20:50
Oil-Col	Colophony	Linseed oil	Rectified turpentine oil	30:20:50
Oil-San	Sandarac standard	Linseed oil	Rectified turpentine oil	30:20:50
Oil-Cop	Manila Copal	Linseed oil	Rectified turpentine oil	30:20:50

Solvent-based varnishes were formulated with 30 wt% of grinded natural resin, dissolved in the appropriate solvent and stirred for 1 h. When needed, an ultrasonic bath was also used in order to speed up the dissolution process.

The linseed oil mixtures (see Table 1) were prepared by heating the oil and the resin in separate pyrex containers using a sand bath (Gerhardt sand bath –type HS). The latter allows a gradual heating with a precision of 5 °C in the range 25-400°C temperature. Linseed oil containing a cobalt drier was chosen to reduce the induction time during the curing process [24].

Colophony and mastic resins were melted, mixed with hot oil (120 °C), and then heated up to 220 °C for about 15 minutes. Sandarac and copal were prepared in a similar way by heating them and the oil up to 150 °C and then the mixtures up to 285 °C. After that, the mixtures were left to cool slowly down to 60 °C then rectified turpentine oil was added in 1:1 ratio (wt:wt). Once cooled, the varnishes were filtered in order to isolate the insoluble residue and hermetically bottled. The yield of mastic and colophony was almost 100 %, while that of sandarac and copal was around 50 % because of the gelatinous residue.

All the formulations were uniformly cast on two different substrates: glass slides (2.6x4.5 cm) for gravimetric measurements, and potassium bromide (KBr) windows for FTIR analysis. Varnishes on glass slides were applied in different amounts (0.8, 0.4, and 0.2 g), in order to evaluate the morphological changes and the weight losses during accelerated photo-ageing.

Curing was formerly carried out on a leveled plane for one month under controlled laboratory conditions. The samples were then put in a ventilated oven at 25°C for 24 h without light, and vacuum dried for about 1 week until a constant weight was reached. This was taken as the starting time (t_0) for the gravimetric measurements.

Additionally, varnishes were applied also on primed linen canvas, constituted of a commercial blend of calcium sulphate and calcium carbonate bound with rabbit skin glue as binding medium. Such substrate was considered very suitable to evaluate the discolouration effects, such as yellowing or bleaching, as a function of irradiation time. The pigment to binder ratio was about 90/10 (wt/wt). Each varnish solution was applied by brush in order to obtain a film thickness of 20-30 µm.

Accelerated ageing

After a curing time of 1 month, all the samples (varnishes applied on KBr discs, glass slides and canvases) were aged in a test chamber (Solarbox 3000e, CO.FO.ME.GRA, Milan, IT) under a cw

air-cooled Xenon Lamp (range 290÷850 nm) in order to simulate direct sunlight radiation. The irradiance was kept at 50 mW/cm² and the temperature of the Black Standard Thermometer (B.S.T) at the surface of the samples did not overreach 50 °C, which is slightly above the glass transition (T_g) temperatures of the present varnishes, but well below those of the thermal breakdown. The artificial ageing was carried out for an overall time of 500 hours.

The infrared transmission and Vis reflectance spectra were collected in order to monitor the ageing process after 0, 20, 34, 52, 77, 102, 125, 150, 200, 252, 347 and 500 hours. Measurements corresponding to time zero refer to those collected after one month from the varnish formulation, when all samples were dry to the touch.

Material characterisation

The ageing effects were investigated mainly using FTIR spectroscopy, which were carried out using a Perkin Elmer mod. System 2000 spectrometer. The infrared spectra were collected in transmission mode between 4000-370 cm⁻¹ with a resolution of 2 cm⁻¹ and 4 scans on the same film casted on KBr window before and after ageing. Special care was dedicated to reposition the KBr discs as reproducibly as possible in the beam path at different ageing times in order to achieve quantitative information. Spectra were plotted in absorbance units (Abs) according to the Lambert-Beer law (Abs=-logT) [25-27] without normalization, baseline corrections or smoothing filters. The photo-oxidative kinetics was hence studied by integrating the absorption bands, total-area, corresponding to the main stretching modes, such those of OH, CH and C=O. For each band the same baseline was taken, ranging between 3700-3100, 3100-2700 and 1900-1550 cm⁻¹, respectively.

Furthermore, gravimetric and colorimetric characterisations were carried out in order to collect possible independent evidences of the polymerization and oxidation effects. The relative weight variation of the coatings as a function of the time, $\Delta W(t)/W_0$, were measured using a microbalance with an accuracy of 0.01 mg.

Colorimetry was carried out on grounded canvas samples using a portable Konica Minolta (CM-700d) spectrophotometer (400-700 nm, spectral resolution of 10 nm). Data were collected through a round target mask of 6 mm diameter and calibration was performed by means of a 99% Spectralon® diffuse reflectance standard. L* a* and b* coordinates, were calculated in SCE mode (specular component excluded) with a 10° degrees standard observer and illuminant D65 according to CIEL*a*b* 1976 color space (CIELAB 1976). Each varnished area was subdivided into 24 sectors within which three shifted measurements (1 mm step) were performed yielding a total of 24 × 3 = 72 measurements. The magnitude of the overall color variation is given by $\Delta E = [(\Delta L)^2 + (\Delta a)^2 + (\Delta b)^2]^{1/2}$ and it was calculated as the average value of 72 measurements carried out on the total varnished area, which was about of 6x9 cm².

RESULTS

Gravimetric measurements

Figure 1 shows the weight variation of the solvent and oil based varnishes at different ageing times on glass plates containing 0.2 g of varnish. For colophony (pre-dissolved in ethanol) we decided to

stop the ageing at 20 h because of its relatively rapid changes in the physical and chemical properties.

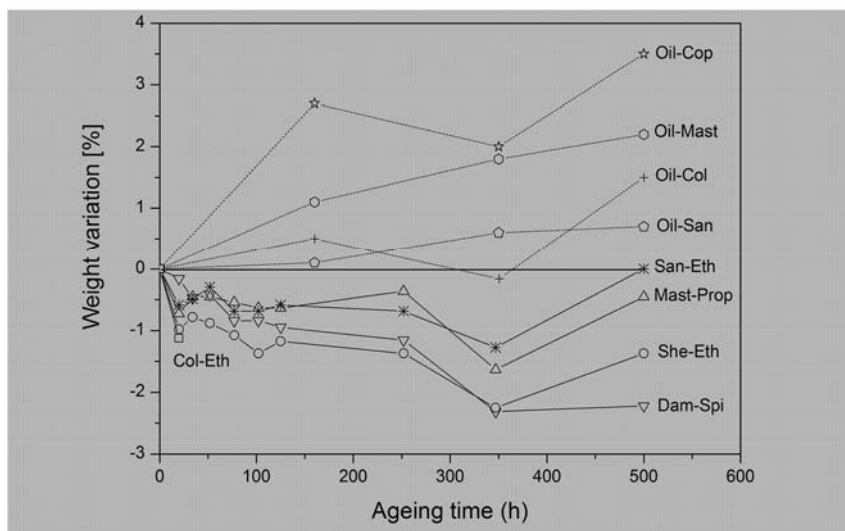


Fig. 1 - Weight variation of varnishes applied on glass as a function of ageing time.

Solvent-varnishes, although preliminarily dried, showed a decrease of weight during the early stages of ageing (after 20 h), which was more pronounced for Col-Eth and She-Eth. Despite the decrease trend has to be reasonable attributed to the loss of solvent residues, such relatively large differences among the different varnishes could be compatible with different degradation patterns. The same solvent was used for sandarac, colophony and shellac, but the weight loss of sandarac was lower than the other two varnishes.

Following the early weight loss, a general and congruent weight modulation was observed for solvent varnishes, which is attributable to the competitive action of oxygen uptake during photo-oxidation against the evaporation of solvent residues. In particular, after 55 h, Dam-Spi, San-Eth and Mas-Prop, showed higher oxygen uptake than shellac according to their propensity to polymerize and cross-link. After longer exposure times (250 h) weight losses got a constant trend, while, a rapid weight drop was detected at about 350 h. In the course of the last ageing cycle (350-500 h), oxidation weight increase started to be predominant for most of the varnishes. At the end of ageing, only for San-Eth the balance between these two components was observed, whereas at the opposite side Dam-Spi exhibited the maximum weight decrease (about -2.3%). The latter result may be interpreted as due to a higher presence of residual white spirit, which “temporary protects” the resin to photo-oxidation and, at the same time, increases the relative weight loss over the time in consequence of its slow evaporation. Such an effect was indeed less pronounced for ethanol and iso-propanol.

Oil-based varnishes showed a general weight increase trend attributable to the rapid oxidation of the polyunsaturated fatty acid chains. Anyway, relative weight modulations were also observed for Oil-Col and Oil-Cop, which are likely due to the presence and/or the formations of volatile components.

1.3.2 Colorimetry

Figure 2 displays the time evolution of $L^*a^*b^*$ coordinates and the total color variation ΔE as a function of the ageing time of both solvent and oil varnish samples.

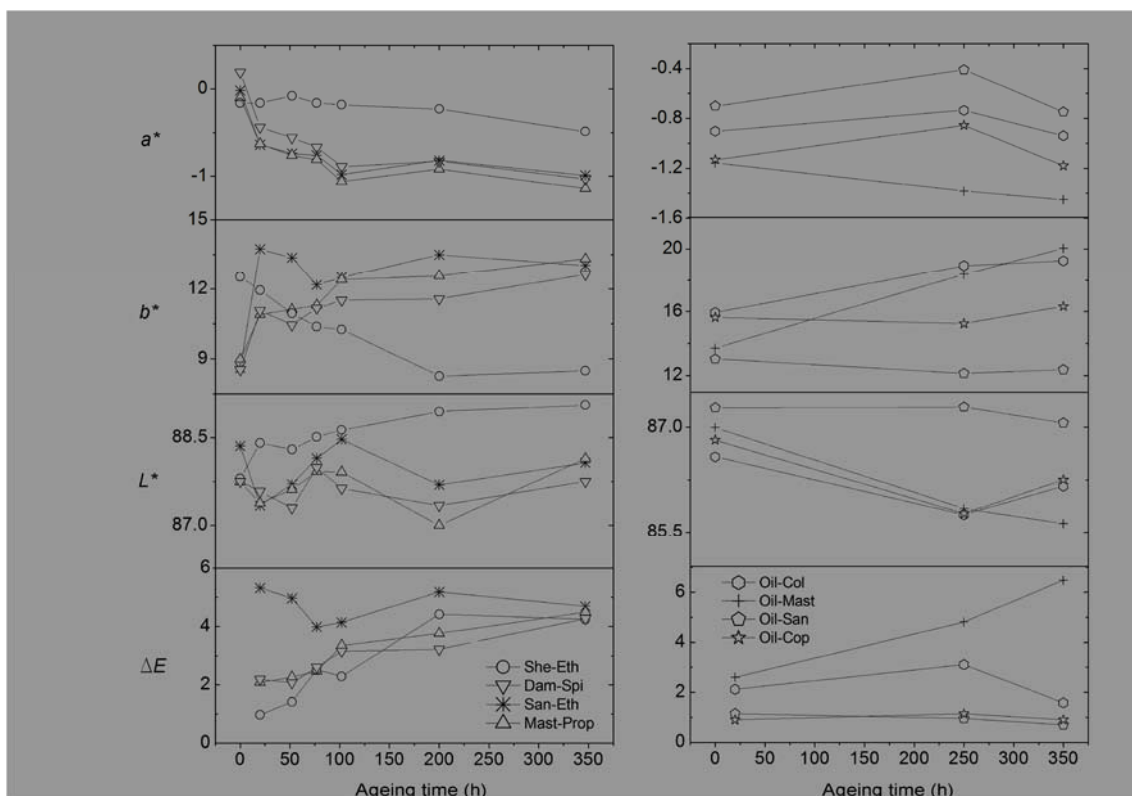


Fig.2 L* a* b* coordinates and ΔE of solvent (left) and oil (right) varnishes as function of the ageing time.

Colorimetric parameters a^* and b^* of solvent varnishes varied between -1.2-0.2 and 9.5-13, respectively. Mas-Prop, Dam-Spi, San-Eth showed a similar discoloration behavior towards the yellow-green direction (increase of b^* and decrease of a^*), whereas a bleaching effect characterized by a significant decrease of b^* and an observable increase of L^* was observed for bleached She-Eth. It is worth noting that the trend for San-Eth was slightly different during the first 50 h. Its rapid yellowing is likely due to a relatively faster oxygen uptake, as observed by the gravimetric measurements (Fig. 1).

After 20 h of exposure Col-Eth (not reported in Fig. 2) showed the following colorimetric variations: $\Delta a^* = +1.93$, $\Delta b^* = +19.44$, $\Delta L^* = -6.95$, and $\Delta E = 18.66$. These significant changes indicate a strong shift toward a deep brown-orange hue, which was evident to the naked eye. For the other solvent-varnishes (Fig. 2) the total color variation was $\Delta E = 4.0$, which can be ascribed mainly to increased b^* (i.e. yellowing), for San-Eth, Mas-Prop, and Dam-Spi, and to decrease of b^* for She-Eth.

The color variations measured for oil-varnishes were in a similar range but different behaviors were observed. a^* parameter for Oil-Mas, Oil-San and Oil-Cop does not significantly change over the irradiation time. On the opposite, Oil-Col undergoes a slight decrease toward the green direction ($\Delta a^* < 0$). The increase of b^* for Oil-Col and Oil-Mas varnishes indicates yellowing effect while Oil-San and Oil-Cop show negligible variations. As regards L^* , Oil-San is brighter and very stable upon irradiation with respect to the other ones, which tend to become slightly darker. As expected, the total color difference was remarkable for the Oil-Col ($\Delta E = 4.0$), according to the behavior of the correspondent solvent-based varnish, while it was negligible for the other oil varnishes.

Photo-induced ageing of terpenoid compounds involved several modifications at molecular level, as shown by transmission FTIR spectroscopy. Specifically, the main interested parts were: the hydroxyl region (2700–3700 cm^{-1}), C-H stretching region (2850–3000 cm^{-1}), carbonyl region (1500–1900 cm^{-1}) and fingerprint region (600–1300 cm^{-1}). A list of the frequency assignments of the absorbing bands, which exhibited ageing changes, are presented in Table 2.

Solvent varnishes

Triterpenoid varnish films: mastic and dammar

Figure 3 displays the FTIR absorption spectra of Mas-Prop and Dam-Chl films, showing the temporal evolution during ageing of the main stretching bands. The Dam-Spi (not shown) followed the same photo-degradation pathway but with a slower oxidation rate (see below).

As shown, the wide O-H stretch vibration increases in intensity and broadens during the overall irradiation time. A noticeable band shift from 3410 to 3440 cm^{-1} and 3417 to 3442 cm^{-1} in light-aged Mas-Prop and Dam-Spi, respectively, was observed. Furthermore, the growth of the shoulder-peaks at about 3230 cm^{-1} and 2600 cm^{-1} , for both the aged triterpenoids resins, could be related to the formation of carboxylic acids groups via condensation reactions [14,17,21]. Carboxylic acid groups also have an increased absorption band in the carbonyl stretching region.

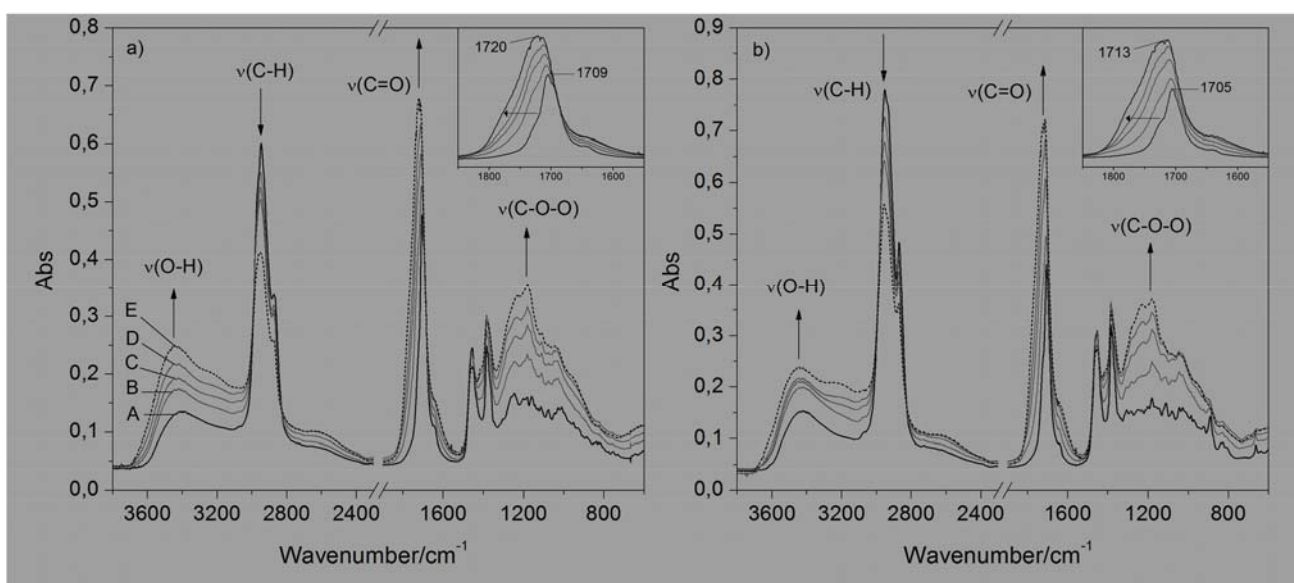


Fig. 3 Transmission FTIR spectra of Mas-Prop (a) and Dam-Chl (b) films at different ageing times (A:0h. B:20h. C:52h. D:102h. E:500h). The arrows indicate the changes of the main vibrational groups induced by the irradiation while in the inset, the shift and the broadening of the carbonyl band are highlighted.

The insets in Fig. 3 show an intensity rise and a significant broadening of the carbonyl C=O stretching bands, assigned to the carbonyl stretching vibration of aldehydes, ketones, and carboxylic acids. Carbonyl band is also shifted toward higher wavenumber of 11 and 8 cm^{-1} for Mas-Prop and Dam-Chl, respectively, which can be related to new intermolecular interactions, as the formation of hydrogen bonds, and most likely new functional groups.

The C=C stretching at 1640 cm^{-1} was only weakly affected by ageing, though it was slightly broadened and enhanced in both the triterpenoid resins. Nevertheless, such modifications do not justify possible isomerization reactions of isolated double bonds into conjugated systems. Other

important modifications displayed in Fig. 3 are in the fingerprint region (600–1300 cm^{-1}). The bands at about 1230 and 1180 cm^{-1} assigned to the stretch vibration of carboxylic and hydroperoxide (COOH and COOOH) bonds are markedly characterized by an increased intensity, in particular way at 1180 cm^{-1} . Additionally, the band at 1244 cm^{-1} in fresh (1-month-old) Mas-Prop shifted to 1234 cm^{-1} , while the same band at about 1240 cm^{-1} was not clearly defined in fresh Dam-Spi at the early stages of ageing. However, it began to increase markedly after 52 hours, becoming more intense after 500 hour and shifted at 1231 cm^{-1} .

Contrarily to this trend, a progressive decreasing in the C-H stretching absorbance of methyl and methylene groups indicating significant molecular changes to the hydrocarbon skeleton under light ageing was observed, which is in agreement with the above mentioned oxidation pathway (hydrogen abstraction). Furthermore, the absorption bands at 2948 and 2956 cm^{-1} in fresh Mas-Prop and Dam-Spi films were both shifted to 2953 cm^{-1} .

Structural information can be argued also from C–H bending vibrations. Particularly, the bands at 1460–1450 cm^{-1} (C–H bending vibration of methyl and methylene groups) underwent a slight decrease in comparison to that of C–H bending of methyl groups at 1385–1380 cm^{-1} indicating a reduction of the latter.

Diterpenoid varnish films: colophony and sandarac

Figure 4 displays the compositional changes observed for the present diterpenic varnishes during accelerated photo-ageing. Despite the present two resins belong to the *Pinaceae* family, they differ in the resinous acids content and hence in their oxidation, polymerization and degradation pathways.

In artificially aged Col-Eth varnish the hydroxyl absorption was higher than in San-Eth and shifted from 3383 to 3418 cm^{-1} without varying its intensity, while the broad weak double structured band at 2641 and 2536 cm^{-1} decreases markedly during the ageing time.

These bands can be related to the O-H stretch hydrogen bonded to carboxylic functional groups and are characteristic absorptions of abietadiene compounds, such as levopimaric, abietic and neoabietic acids [27-28]. This feature was not observed in San-Eth because this is mainly constituted of labdanes and pimaranes resin acids. Nevertheless, the OH absorption in fresh San-Eth resulted almost negligible and increased strongly during ageing.

On the opposite, C-H stretching bands of methyl and methylene groups decreased slightly in both the diterpenic present resins, even though colophony showed a slower degradation kinetics; the maximum intensity drops from 0.7 to 0.6 Abs units (14%) for Col-Eth and from 0.4 to 0.3 (25%) for San-Eth. The methylene bands at 2932 and 2870 cm^{-1} underwent a major change for the latter whereas they remained almost unvaried in Col-Eth.

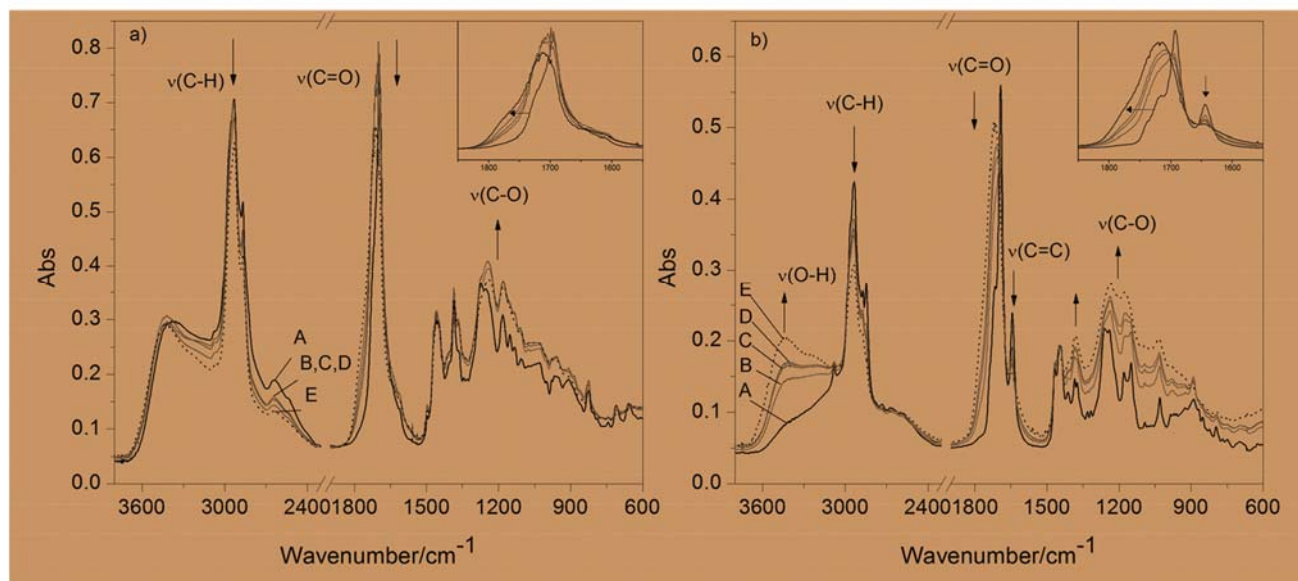


Fig. 4 FTIR transmission spectra of Col-Eth(a) and San-Eth (b) films at different ageing times (A:0h. B:20h. C:52h. D:102h. E:500h). The arrows indicate the changes of the main vibration groups induced by the irradiation while those of the carbonyl band are displayed in the insets.

Significant modifications were observed in the carbonyl stretching region (see the inset in Fig. 4). First of all, the maximum shifted of about $8\text{-}10\text{ cm}^{-1}$ to higher wavenumber for both the resins and the band became broader, in San-Eth more than in Col-Eth. The band of the carboxylic acid group at about 1700 cm^{-1} detected in fresh films (1-month-old) progressively disappeared, while the shoulder at about 1720 cm^{-1} increased after ageing together a new one at about 1770 cm^{-1} indicating the formation of new molecular species, such as ketones, esters and lactones.

Concerning the C=C bond region, the absorption of the band at 1610 cm^{-1} in colophony was very low and its changes negligible. On the contrary, for San-Eth the bands at 1640 and 888 cm^{-1} , which are ascribable to the C=C stretching of unconjugated olefin in the side chain and to the out-of-plane deformation of the exocyclic methylene groups, respectively, resulted drastically reduced at the end of ageing. These two bands along with that attributed to CH ethylenic stretchings at 3080 cm^{-1} are representative of labdatriene molecules, such as communic acid [18-19-29]. The opening of the C=C bonds and the increase of the peaks at 1384 and 1449 cm^{-1} (bending deformation of methyl groups and to the scissoring deformation of methylene groups, respectively), can be used to monitor the development of cross linking in San-Eth varnish.

A further change observed was the intensity increases in the region $1300\text{-}1000\text{ cm}^{-1}$. The most important ones, evidenced in San-Eth, were a slight increase of the bands at about 1250 cm^{-1} (C-O stretching) and 1180 cm^{-1} (C-C-O in peroxides). They changed in the early stage (20 h) of ageing and were likely due to presence of new oxidized compounds (peroxides, acids, esters and lactones).

Shellac

Figure 5 reports the sequence of spectra for non-aged and artificially aged She-Eth films. All of them exhibited changes of peak intensities while broadening was lower than for other resins.

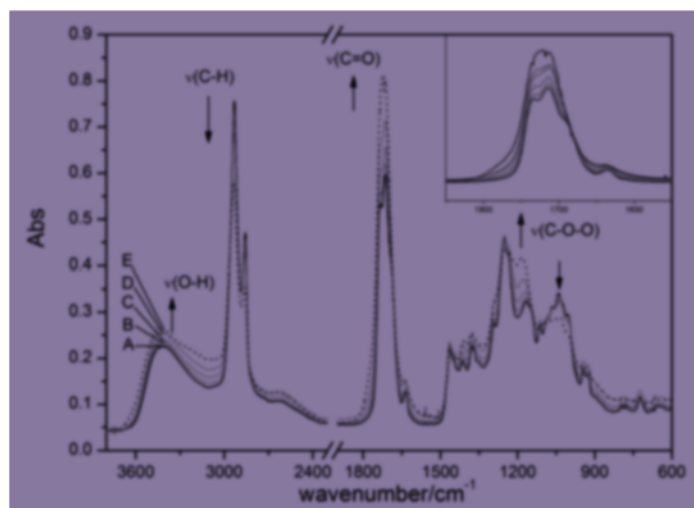


Fig. 5 Transmission FTIR spectra of She-Eth varnish film (pre-dissolved in ethanol) at different ageing times (A: 0h. B: 20h. C: 50h. D: 100h., E: 500h). The arrows indicate the changes of the main vibration groups induced by the irradiation while in the inset reports a detail of the carbonyl stretching region.

Here, a slight increase in the OH stretching region due to the presence of hydroxyl and carboxylic groups has been observed. C-H stretching and bending bands decreased. At the same time, the bands at 1415 and 1377 cm^{-1} increased in intensity and slightly shifted in wavenumber, suggesting structural deformations in the region of skeletal vibrations.

These changes reflect what observed in the carbonyl stretching region. The band of the carboxylic groups at 1715 cm^{-1} and the shoulders at about 1690 and 1735 cm^{-1} were modified over the ageing time, as clearly shown in Fig. 5. An overall band increase is observed which led to an overlapping of the different signals, making difficult their discrimination. In any way, the overall intensity increase and shift toward higher wavenumber, suggests the formation of ester groups, as demonstrated by the broadening of carbonyl band at 1780 cm^{-1} due to the possible formation of cyclic esters (e.g. lactides or lactones). The signal of C=C bond deriving from shellolic and jalaric acids, was the little band at 1640 cm^{-1} which tends to be reduced during the ageing.

Other important features that further support the highlighted changes in the carbonyl region were in the 1300-900 cm^{-1} range. The C-H scissoring band ($\delta_s \text{CH}_2$) of the aliphatic chain at 1464 cm^{-1} does not undergo significant changes. The most relevant ones regard the continuous increase of the C-O stretching of the ester bonds at 1171 cm^{-1} along with the reduction of the C-C-O stretching of the alcoholic group at 1035 cm^{-1} . These spectral features suggest clearly the cross-linking process was driven by self-esterification. The starting point of such process may be related to the dissociation of aldehydic and carboxylic acid functions present in jalaric acid. A similar trend has been detected during thermal ageing by Farag [3,23, 30, 31].

Table 2 – Infrared absorption peaks of solvent varnishes as naturally cured (1 month-old) and artificially aged (500 h) films. Bands exhibiting intensity variations are indicated in italics while the abbreviation sh refers to the shoulder peaks. Frequencies are given in wavenumber/cm⁻¹.

Naturally dried films					Artificially aged films					Approx Assignment ^a
Mas-Pro	Dam-Spi	Col-Eth	San-Eth	She-Eth	Mas-Pro	Dam-Spi	Col-Eth	San-Eth	She-Eth	
3410	3417	3383	3400sh	3417	<i>3440</i>	3442	<i>3418</i>	<i>3441</i>	<i>3423</i>	v(O-H)
--	--	--	--	--	<i>3227sh</i>	<i>3213sh</i>	--	<i>3244sh</i>	--	v(O-H)
3074	3071	3078	3080	--	--	--	<i>3076</i>	--	--	v(C=CH) olefinic
--	--	2953sh	2962sh	--	--	--	<i>2956sh</i>	--	--	v _{as} (CH ₃)
2948	2956	2932	2934	2932	<i>2953</i>	<i>2953</i>	<i>2930</i>	<i>2940</i>	<i>2934</i>	v _{as} (CH ₂)
2877	2873	2870	2873	2858	<i>2874</i>	<i>2870</i>	<i>2869</i>	<i>2877sh</i>	<i>2860</i>	v _s (CH ₃)
--	--	--	2847	--	--	--	--	<i>2850sh</i>	--	v _s (CH ₂)
2600	2600sh	2640	--	2642sh	<i>2600sh</i>	<i>2636sh</i>	<i>2640sh</i>	<i>2600sh</i>	<i>2641sh</i>	--
--	--	2540	--	--	--	--	--	--	--	--
--	--	--	--	--	<i>1776sh</i>	<i>1773sh</i>	<i>1780sh</i>	--	--	v(C=O), cyclic esters
--	--	--	1735sh	--	--	--	--	<i>1735sh</i>	--	v(C=O)
--	--	1720sh	1716sh	1732	--	<i>1721</i>	--	--	<i>1720</i>	v(C=O)
1709	1705	1695	1693	1713	<i>1720</i>	<i>1713</i>	<i>1713</i>	<i>1713</i>	<i>1713</i>	v(C=O)
1649sh	1645	--	1644	1637	<i>1649sh</i>	<i>1651sh</i>	--	--	<i>1643</i>	v(C=C)
--	--	1611sh	--	--	--	--	1611sh	--	--	v(C=C) aromatic ring
--	--	1495	--	--	--	--	1495	--	--	--
--	1460	--	1469	1465	--	1461	--	--	1461	δ _s (CH ₂)
1457	1455	1460	1449	--	<i>1450</i>	1454	<i>1455</i>	1451	--	δ _{as} (CH ₃)
--	--	--	--	1414	1415	--	--	--	<i>1415</i>	δ(O-H)
1385	1384	1385	1384	--	<i>1385</i>	<i>1385</i>	1383	<i>1383</i>	--	δ(CH ₃)
--	1377	1366	1374	1375	--	--	<i>1365</i>	--	<i>1378</i>	δ _s (CH ₃)
--	--	--	--	1293	--	--	--	--	<i>1293sh</i>	v(C-O)
--	--	1273	1261	--	--	--	<i>1270sh</i>	--	--	--
1244	--	1250	1240	1252	<i>1234sh</i>	<i>1231</i>	1240	<i>1235</i>	1250	v(C-C), ω,τ(C-H), v(C-O-O)
1180	1181	1180	1179	1167	<i>1180</i>	<i>1181</i>	<i>1178</i>	<i>1176</i>	<i>1180</i>	ω,τ(C-H), v(C-O-O)
1158	--	1152	1150	1142sh	--	--	--	--	--	--
--	--	1131	--	--	--	--	<i>1131sh</i>	--	--	--
1113	1111	1106	--	1114	1108	--	<i>1106sh</i>	--	--	--
--	--	--	1031	--	--	--	--	<i>1034</i>	--	--
1076	1079	1084	--	--	--	--	--	--	--	v(C-O), v(C-C)
1029	1042	1047	--	1040	<i>1047</i>	<i>1048</i>	--	--	<i>1035</i>	v(C-O), v(C-C)
--	--	--	--	1000	--	--	--	--	<i>998sh</i>	---
947	--	--	--	945	<i>947sh</i>	--	--	--	<i>946</i>	ω,τ(C-H)δ(O-H) "oop"
--	--	--	--	927	--	--	--	--	<i>930</i>	ω,τ(C-H)δ(O-H) "oop"
--	--	896	--	899	--	--	--	--	--	--
--	--	879	--	--	--	--	--	--	--	--
--	--	824	--	--	--	--	825	--	--	--
--	757	--	--	796	--	--	--	--	796	--
--	--	--	--	780	--	--	--	--	780	--
--	--	710	--	723	--	--	--	--	725	γ(CH ₂)
--	--	657	--	--	--	--	--	--	--	--
--	890	880	890	--	--	--	--	--	--	δ(C-H)

^av: stretching; δ: bending; ω: wagging; τ = twisting; γ: rocking; as: asymmetric; s: symmetric

Oilvarnishes

The first step was to verify the chemical changes of the prepared oil-resin mixtures after the thermal treatment needed for their formulation. In this way, possible intermolecular interaction between the resin and oil and the influence of the heat processing on the end-products was evaluated. Thereafter, for each type of oil varnish the light-induced effects during ageing were evaluated, as previously described for solvent-based varnishes.

Oil-Mas mixture was heated between 120-220 °C, which is above the typical softening and melting thermal thresholds of the triterpenoid resins. Spectral features of the end-product along with those of fresh mastic and linseed oil samples are displayed in Fig. 6, while bands assignment is listed in Table 3.

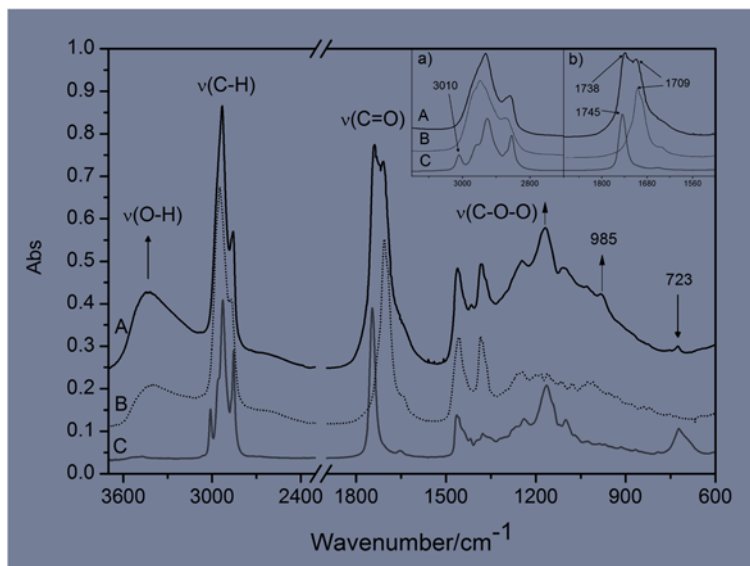


Fig. 6 Transmission FTIR spectra of linseed Oil-Masvarnish (A), fresh mastic (B), and linseed oil (C) after 1 month of natural curing. The insets show the CH (a) and C=O (b) stretching regions.

The first important modification observed after cooking was the increase of hydroxyl groups (broad band centered at 3440 cm^{-1}), which comes both from the added mastic resin and from the extensive oxidation occurring during heating [14]. The disappearance upon heating of the band at 3010 cm^{-1} (see the inset in Fig. 6) and the decreasing of the out-of-plane CH bending vibration in non-conjugated cis olefin at 723 cm^{-1} , both assigned to linseed oil, suggest a partial saturation of the double bond associated to isomerization. The isomerization reaction can be justified with the appearance of a new band at 985 cm^{-1} , assigned to out-of-plane C-H bending vibrations in non-conjugated or conjugated trans double bonds.

Fresh linseed oil and mastic resin show C-H stretching vibrations at 2927 and 2948 cm^{-1} , respectively. After heating, these signals became a single broad band (see the inset in Fig. 6) with a maximum centered at 2931 cm^{-1} , which is the resultant of the combination of the two peaks.

A double structured band has been indeed detected in the carbonyl region due to the presence of both the components. In detail, the intense carbonyl band of the ester linkages at 1745 cm^{-1} of the linseed oil was shifted at 1738 cm^{-1} after heating. On the opposite, the other one at 1709 cm^{-1} did not change and it can be attributed to the carbonyl band of aldehydes, ketones and carboxylic acids of mastic resin. This suggests that both the components after thermal treatment conserve their own carbonyl absorption features. Nevertheless, a considerable broadening was detected, which is congruent with the formation of both saturated and acidic compounds. In particular, the weak bands of C=C bond at 1654 cm^{-1} in fresh linseed oil and at 1640 cm^{-1} in mastic, which are sheltered by the broadening of the carbonyl peaks in the oil-resin mixture, probably underwent some modifications during the heat processing, as observed also for the out-of-plane deformation at 722

cm^{-1} of linseed oil [34-35]. However, no notable increase in the vibration bands of conjugated carbon double bonds was detected.

Further interesting remarks upon heat processing can be also noticed in the fingerprint region $1600\text{--}600\text{ cm}^{-1}$. With regards to the CH bending bands, the spectrum of Oil-Mas shows two bands at 1460 and 1380 cm^{-1} , which are the combination of the C-H bending vibrations of the terpenoid resins and linseed oil. However, an overall intensity increase in the $1300\text{--}1000\text{ cm}^{-1}$ is observed. This increase is mainly due to the vibrations of C-O, C-C and C-H bonds in linseed oil, although the formation of small amounts of hydroperoxides may contribute to the signal intensity in this region.

Photo-oxidation of mastic oil varnish

In Fig. 7 FTIR spectra of Oil-Mast different ageing times have been compared. The assignments and the most relevant changes in band position are reported in Table 3. Significant spectral differences were detected since short times (20 h) of light ageing.

The signal intensity of CH stretching decreased of about 15% after 100 h of artificial solar light irradiation and a further 20% decrease was observed between 100-500 h, indicating a fast and significant hydrogen abstraction on methylene group both in fatty acids chain and polycyclic triterpenoid acids. This is in agreement with an oxidative chain cleavage reaction known to yield volatile oxidation products [36] and also with what observed in mastic resin.

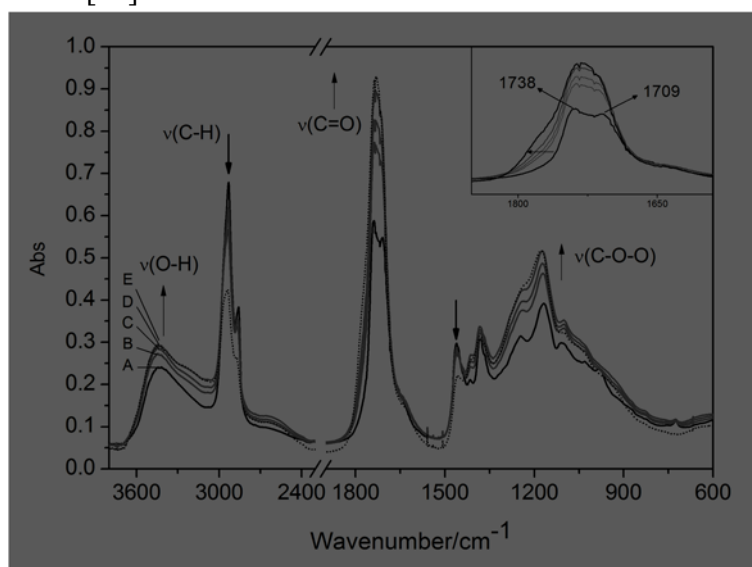


Fig. 7 Transmission FTIR spectra of Oil-Mas (cured) at different ageing times (A:0h; B:20h; C:50h; D:100h; E:500h). The arrows show the changes of the main vibrational groups induced by the irradiation while the inset, those ones in the carbonyl region.

The intense decreasing of CH stretching peak at 2932 cm^{-1} was accompanied by a shift toward 2940 cm^{-1} and an interesting change of its secondary peak, which decreased and moved from 2858 to 2876 cm^{-1} , in accordance with a decrease of $-\text{CH}_2$ groups and relative increase of the $-\text{CH}_3$ ones. The latter frequency (2876 cm^{-1}) is closer to that of the mastic resin, as well as the drastic decreasing of the C-H bending ($\delta_s -\text{CH}_2$) at 1460 cm^{-1} . As previously observed, this latter band has in fresh mastic an intensity similar to that at 1380 cm^{-1} and tends to become lower after exposure to intense radiation. As reported by Lazzari [34], prolonged exposure times of linseed oil generate exactly the same decreasing at 1460 cm^{-1} .

Table 3 – Assignment of the infrared absorption peaks (cm^{-1}) after the heat processing (pre-heated) and artificial ageing (light aged) of linseed oil-mastic films. For comparison purposes fresh linseed oil and mastic films have been also reported. Bands which change in intensity after the light ageing treatment are indicated in *italics* while the abbreviation sh corresponds to shoulder peaks.

Linseed oil	Assignment ^a	Mastic	Assignment ^a	Oil- Mas (pre-heated)	Oil-Mas (light aged)
--	--	3410	$\nu(\text{O-H})$	3440	<i>3448</i>
3009	$\nu(\text{C-H})=\text{CH}$	--	--	--	--
2960 sh	$\nu_a(\text{C-H})\text{CH}_3$	2966sh	$\nu_a(\text{C-H})\text{CH}_3$	--	<i>2960sh</i>
2927	$\nu_a(\text{C-H})\text{CH}_2$	2948	$\nu_a(\text{CH}_2)$	2931	<i>2940</i>
--	--	--	--	2870sh	--
2856	$\nu_s(\text{C-H})\text{CH}_2$	2877	$\nu_s(\text{CH}_3)$	2858	<i>2876</i>
--	--	2600sh	--	2600sh	<i>2600sh</i>
--	--	--	--	--	<i>1780sh</i>
1745	$\nu(\text{C=O})$ ester	1709	$\nu(\text{C=O})$	1741	<i>1731-36</i>
--	--	--	$\nu(\text{C=O})$	1709	<i>1714sh</i>
--	----	1640	$\nu(\text{C=C})$	1640sh	<i>1640</i>
1654	$\nu(\text{C=C})$ of <i>cis</i> -CH=CH-	1455sh	$\nu_{as}(\text{CH}_3)$	1455sh	<i>1455</i>
1464	$\delta_{as}(\text{CH}_3)$, $\delta(\text{CH}_2)$	1457	$\delta_s(\text{CH}_2)$, $\delta_{as}(\text{CH}_3)$	1460	<i>1460</i>
1418	$\delta_s(\text{CH}_2)-\text{CH}_2-\text{CO}-\text{O}-$	--	--	1415	<i>1415sh</i>
1378	$\delta_s(\text{CH}_3)$	1385	$\delta(\text{CH}_3)$	1380	<i>1380</i>
1238	$\nu_a(\text{C-O})$ in ester	1244	$\nu(\text{C-C}), \delta(\text{C-O-O})$	1247	<i>1240sh</i>
--	--	1180	$\omega, \tau(\text{C-H}), \nu(\text{C-O})$	--	<i>1177</i>
1164	$\nu_a(\text{C-O})$ in ester	1158	--	1166	--
--	--	1113	$\delta(\text{C-H})$	1110	--
1100	$\nu_a(\text{O-CH}_2-\text{C})$	1076	$\delta(\text{C-H}), \nu(\text{C-O})$	1100	<i>1100sh</i>
--	--	1029	$\delta(\text{C-H}), \nu(\text{C-O})$	1030	--
--	--	--	$\omega, \tau \text{ CH}=\text{CH trans}$	985	--
723	$\gamma-(\text{CH}_2)-\text{wag}(\text{C-H})=\text{CH}$	--	$\omega, \tau \text{ CH}=\text{CH cis } \gamma-(\text{CH}_2)$	725	--

^a ν : stretching; δ : bending; ω : wagging; τ = twisting; γ : rocking; as: asymmetric; s: symmetric

Additional ketone, ester and acid carbonyls were formed during photo-oxidative polymerization. The double structured shape of carbonyl disappeared and transformed into a new one given by a sum of several undistinguishable contributions (see Fig. 7). These changes reflect the formation of ester linkages between the two components, as evidenced by the increase of the characteristic absorbances at 1239, 1174 and 1100 cm^{-1} . The shoulder around 1715 cm^{-1} could suggest the formation of carbonyl products such as δ lactones (six membered ring) with probable unsaturation in α to C=O. A further important change observed was the broadening and the increased shoulder at 1780 cm^{-1} , which indicates the formation of secondary oxidation products, such as γ lactones (five membered ring) and anhydrides both in oil and resin [15, 36-37]. The formation of anhydrides and lactones represents the final stages of cross-linking and occurs via dehydration reaction of carboxylic acids or carboxylic acids and alcohols, respectively. Broadening of carbonyl band and the formation of lactones was very pronounced also in artificially aged mastic without oil. For comparison purposes, spectra of mastic and mastic-linseed oil mixture are shown in Fig. 8.

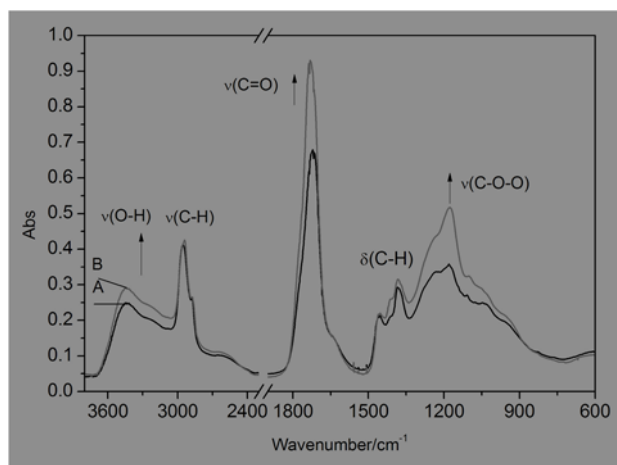


Fig. 8 Transmission FTIR spectra of mastic (A) and oil-mastic mixture (B) after 500h of accelerated lighting conditions.

Typically, the most relevant changes reside in the higher intensity of OH, C=O and C-O stretching groups due to the high content of primary oxidation products deriving from polyunsaturated acids such as: allyl hydroperoxides, chemical moieties containing both allyl ($-\text{CH} = \text{CH}-\text{CH}_2-$) and hydroperoxide ($-\text{OOH}$) groups as in $-\text{CH} = \text{CH}-\text{CH}(\text{OOH})$. Nevertheless, the intensity changes do not allow the identification of the oil component in the mixture, although the carbonyl band appears at higher wavenumber (1735 cm^{-1}) with respect to the aged mastic (1720 cm^{-1}).

Other minor features that could be representatives for identifying the oil were transformed both during thermal treatment and photo-oxidation, thus adding new drawbacks in recognizing the oil.

Oil-colophony varnish

The infrared spectrum of Oil-Col mixture after the heat processing (heated up to 120° for 1 h) is shown in Fig. 9 and the changes in band position are listed in Table 4.

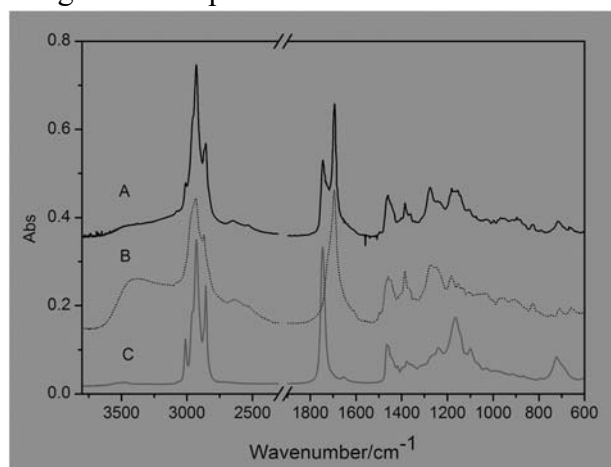


Fig. 9 Transmission FTIR spectra of Oil-Col varnish (A) after 1 week of natural curing (heated at 120°C). For a qualitative comparison fresh colophony (B) and linseed oil (C) spectra are also reported (offset).

As observable in Fig. 9, the OH stretching band of carboxylic acids was less intense with respect to pure colophony, most probably because of the dehydrogenation of abietic acid produced by the thermal treatment [38]. Contrarily to Oil-Mas, Oil-Col preserved several spectral features related to

the presence of the oil phase in the mixture, such as those of C-H stretching region which exhibited the same shape and bands position of linseed oil (see Table 4).

Nevertheless, the characteristic stretching of the vinyl function in labdatriene molecules (at 3078 cm^{-1}) and the two bands at 2640 and 2535 cm^{-1} allowed discriminating the contribution of the colophony resin.

As for Oil-Mas, the carbonyl region was structured by the superposition of the 1740 (oil) and 1694 cm^{-1} (colophony) peak. Shape and band positions suggest that any interaction between the two components took place due to the heating process. The higher intensity of C-H groups in the mixture, in comparison to the unheated references (oil and resin), is due to the addition of turpentine. Conversely, the carbonyl peaks were separated of about 50 cm^{-1} and then well-resolved. The weak signal of C=C bonds makes difficult their discrimination or the assessment of possible changes upon thermal treatment. The bending of methyl and methylene groups did not show relevant changes, as well as the overall intensity between 1300 and 900 cm^{-1} . This suggests that the peroxides formation did not take place during heating but most likely, a loss of volatile compounds occurred. Concerning the identification of the type of oil varnish, at this degree of curing, all the spectral features of both the components were clearly detectable.

Photo-oxidation of colophony oil varnish

First of all, some modifications before the xenon lamp exposure were noticed. In Fig.10 the spectrum B corresponds to the Oil-Col mixture after 1 month of natural curing (t_0), which evidences a rapid oxidation reaction, leading to the increase of the carbonyl and hydroxyl groups and the decrease of the CH_2 and CH_3 groups (complete disappearance of *cis* unsaturation). This indicates that, light, oxygen and driers catalyze the hydrogen abstraction from the methylene groups very quickly. This leads to conjugated and non-conjugated hydroperoxides (increase in the $1300\text{-}1000\text{ cm}^{-1}$), which via radical recombination produce cross-linking (alkyl, ether or peroxy bridges).

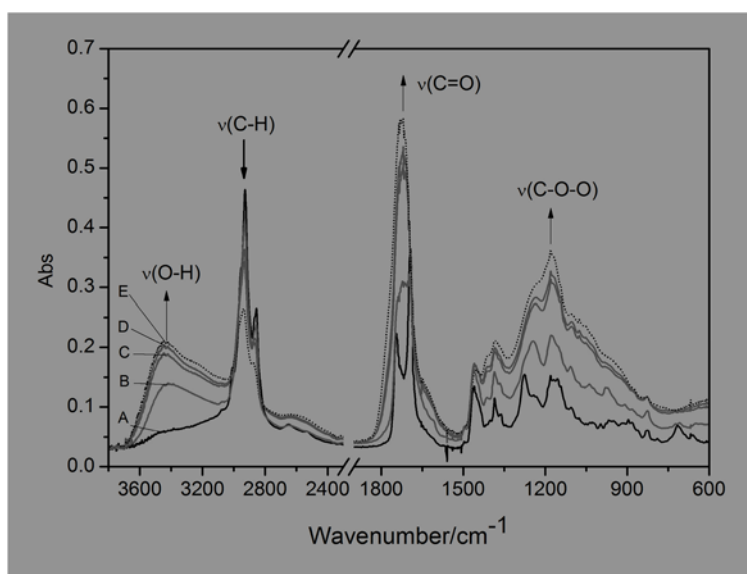


Fig. 10 Transmission FTIR spectra of Oil-Col at different ageing times (A: after 1 week. B: 0h. C: 25h. D: 50h. E: 500h). The arrows indicate the main changes observed.

Table 4 Assignment of the absorption peaks (cm^{-1}) after the heat processing (pre-heated) and artificial ageing (light aged) of linseed oil-colophony film. For a qualitative comparison fresh linseed oil and colophony films have been also reported. Bands which change in intensity after the light ageing treatment are indicated in *italics* while the abbreviation sh corresponds to shoulder peaks.

Linseed oil	Assignment ^a	Coloph.	Assignment ^a	Oil-Col (pre-heated)	Oil- Col (light aged)
--	--	3383	$\nu(\text{O-H})$	3480sh	<i>3432</i>
--	--	--	--	--	<i>3240sh</i>
--	--	3078	$\nu(\text{C=CH})$	3078	3078
3009	$\nu(\text{C-H})=\text{CH}$	--	--	3009	--
2960 sh	$\nu_{\text{as}}(\text{C-H})\text{CH}_3$	2953sh	$\nu_{\text{as}}(\text{CH}_3)$	2957sh	--
2927	$\nu_{\text{a}}(\text{C-H})\text{CH}_2$	2932	$\nu_{\text{as}}(\text{CH}_2)$	2927	<i>2936</i>
2856	$\nu_{\text{s}}(\text{C-H})\text{CH}_2$	2870	$\nu_{\text{s}}(\text{CH}_3)$	2857	<i>2872</i>
--	--	2640	$\nu(\text{O-H})$	2640	--
--	--	2540	$\nu(\text{O-H})$	2535	<i>2560sh</i>
1745	$\nu(\text{C=O})$ ester	--	$\nu(\text{C=O})$	1745	<i>1740sh</i>
--	--	1720sh	$\nu(\text{C=O})$	--	<i>1730</i>
--	--	1695	$\nu(\text{C=O})$	1695	--
1654	$\nu(\text{C=C})$ of <i>cis</i> -CH=CH-	--	--	--	--
--	--	1610sh	$\nu(\text{C=C})$ <i>cis</i> + aromatic ring	1610sh	<i>1620sh</i>
--	--	1495	aromatic ring	1495	--
1464	$\delta_{\text{as}}(\text{CH}_3)$, $\delta(\text{CH}_2)$	1460	$\delta(\text{CH}_2)$, $\delta(\text{CH}_3)$	1460	<i>1450</i>
1418	$\delta_{\text{s}}(\text{CH}_2)$ -CH ₂ -CO-O-	--	--	--	<i>1412sh</i>
1378	$\delta_{\text{s}}(\text{CH}_3)$	1385	$\delta(\text{CH}_3)$	1385	<i>1385</i>
--	--	1366	$\delta(\text{CH}_3)$	--	--
--	--	1273	$\nu(\text{C-C})$, $\delta(\text{C-H})$	1273	--
1238	$\nu_{\text{as}}(\text{C-O})$ in ester	1250	$\nu(\text{C-O})$	1240	<i>1232sh</i>
--	--	1180	$\delta(\text{C-H})$, $\nu(\text{C-O})$	1180	<i>1180</i>
1164	$\nu_{\text{as}}(\text{C-C-O})$ in ester	1152	--	1166	<i>1160sh</i>
--	--	1131	$\delta(\text{C-H})$	1110	<i>1142sh</i>
1100	$\nu_{\text{as}}(\text{O-CH}_2\text{-C})$	1106	$\delta(\text{C-H})$, $\nu(\text{C-O})$	1100	<i>1100</i>
--	--	1084	$\delta(\text{C-H})$, $\nu(\text{C-O})$	1100	<i>1075</i>
--	--	1047	$\delta(\text{C-H})$, $\nu(\text{C-O})$	1030	--
--	--	--	ω , τ CH=CH trans	985	--
--	--	824	--	824	<i>824</i>
723	$\gamma(\text{CH}_2)$ -+ ω , τ (C-H) in CH=CH <i>cis</i>	--	ω , τ CH=CH trans	725	--
--	--	707	--	717	--
--	--	658	--	660	--

^a ν : stretching; δ : bending; ω : wagging; τ = twisting; γ : rocking; as: asymmetric; s: symmetric

Oil sandarac and Manila copal varnishes

The spectral evolution of Oil-Cop during ageing was the same as that of Oil-San shown in Fig. 11. Despite the significant temperature rise (285 °C) all the spectral features of the independent components were preserved. The only difference is the relative intensity of the CH₂ and C=O signals that, as in the case of Oil-Col, is due to the presence of turpentine added for the preparation of the mixture. As already shown, the most relevant change was that of the linseed oil phase, which underwent a drastic decrease of *cis* unsaturation (3009 cm^{-1}).

For the resin component the C=C bonds were clearly detectable through the weak absorption of the olefinic group at 3080 cm^{-1} and the most intense ones at 1643 cm^{-1} , which is related to molecules containing pimarane and labdane skeletons. These functional groups are converted into single bonds during the cross-linking and hence their presence suggests that polymerization reactions did not take place yet. The intensity of carbonyl absorption was reduced if compared with the band at 1643 cm^{-1} . This likely arose from the thermal treatment, which led to additional decarboxylation and fragmentation of polycommunic acid. On the other hand, the latter represents a highly cross-linked fraction conferring the typical hardness of such diterpenic resins [18-39].

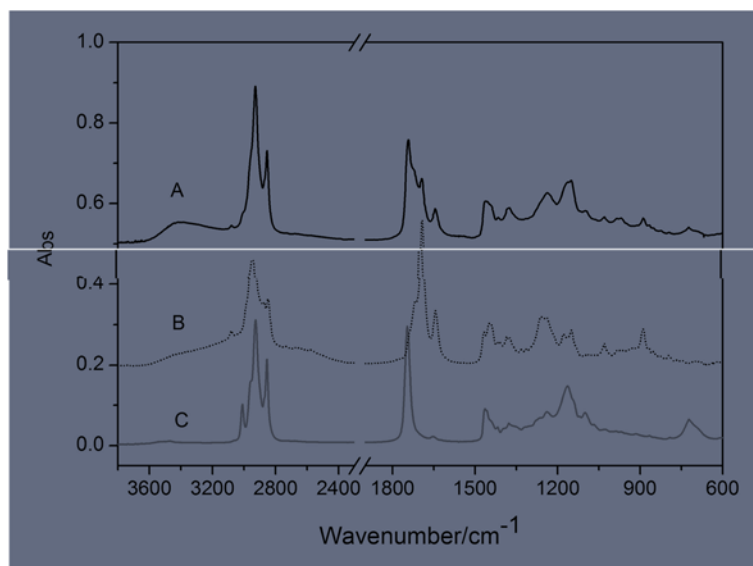


Fig. 11 FTIR transmission spectra of Oil-San varnish (A) after 1 week of natural curing (heated at 285 °C). For a qualitative comparison fresh sandarac (B) and linseed oil (C) spectra are also reported (offset).

Photo-oxidation of Sandarac and Manila copal-oil varnishes

The ageing spectra of Oil-San and Oil-Cop are reported in Fig. 12. These show that mixtures underwent similar polymerization and degradation processes. In fact, assignment and changes in band positions listed in Table 5 can be considered the same for both the diterpenoid resins.

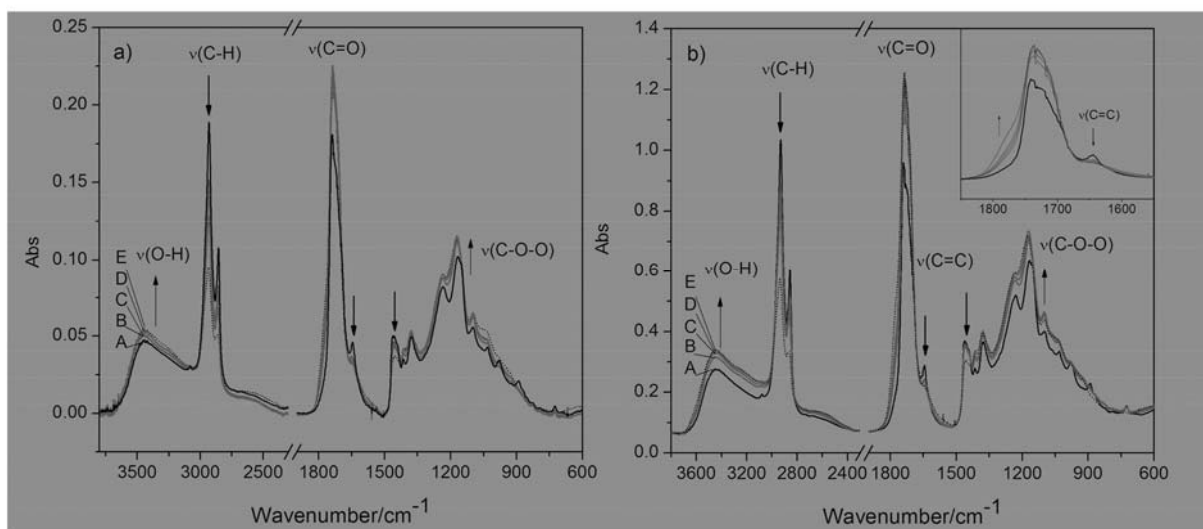


Fig. 12 FTIR transmission spectra of Oil-San (a) and Oil-Cop (b) at different ageing times (A: 0h. B: 25h. C: 50h. D: 100h. E: 500h). The arrows highlight the main changes.

Polymerization and cross linking can be seen and monitored through the significant reduction of the signal intensity of the C=C at about 1645 cm^{-1} , the disappearance of the out of plane deformation of $-\text{CH}_2$ at 889 cm^{-1} along with the drastic intensity decrease of the C-H stretching at 2930 cm^{-1} and the scissoring deformation of methylene groups at about 1460 cm^{-1} . The peak around 1460 cm^{-1} was also shifted (from 1464 to 1454 cm^{-1}). The latter, although less evident, was observed in some pure varnishes (colophony, mastic, sandarac) under UV irradiation, but not in dammar.

Table 5 Absorption peaks assignment (cm^{-1}) of linseed oil-sandarac film after the heat processing (pre-heated) and artificial ageing (light aged). Linseed oil-Manila copal mixture exhibited the same spectral features. For a qualitative comparison fresh linseed oil and sandarac films have been also reported. Band changes are highlighted in *italics* while the abbreviation sh corresponds to the shoulder peaks.

Linseed oil	Assignment ^a	Sand.	Assignment ^a	Oil-San (pre-heated)	Oil-San (light aged)
--	--	3400sh	$\nu(\text{O-H})$	3480sh	<i>3440</i>
--	--	3080	$\nu(\text{C=CH})$ vinyl	3078	--
3009	$\nu(\text{C-H})=\text{CH}$	--	--	3009sh	--
2960 sh	$\nu_{\text{as}}(\text{C-H})\text{CH}_3$	2962sh	$\nu_{\text{as}}(\text{CH}_3)$	2960sh	--
2927	$\nu_{\text{as}}(\text{C-H})\text{CH}_2$	2934	$\nu_{\text{as}}(\text{CH}_2)$	2929	2933
---	--	2873	$\nu_{\text{s}}(\text{CH}_3)$	2870sh	--
2856	$\nu_{\text{s}}(\text{C-H})\text{CH}_2$	2847	$\nu_{\text{s}}(\text{CH}_2)$	2855	2860
--	--	--	--	--	1780
1745	$\nu(\text{C=O})$ ester	--	$\nu(\text{C=O})$	1742	1740
--	--	1716sh	$\nu(\text{C=O})$	1720sh	1720sh
--	--	1693	$\nu(\text{C=O})$	1694	--
1654	$\nu(\text{C=C})$ of <i>cis</i> -CH=CH-	1643	$\nu(\text{C=C})$ <i>cis</i>	1643	1643sh
--	--	1495	aromatic ring	1495	--
1464	$\delta(\text{CH}_3)$, $\delta(\text{CH}_2)$	1469	$\delta(\text{CH}_2)$, $\delta(\text{CH}_3)$	1464	1454
1443sh	$\delta(\text{CH}_3)$, $\delta(\text{CH}_2)$	1449	$\delta(\text{CH}_2)$, $\delta(\text{CH}_3)$	1442sh	--
1418	$\delta_{\text{s}}(\text{CH}_2)$	1412	--	1416	1415
1378	$\delta_{\text{s}}(\text{CH}_3)$	1385	$\delta(\text{CH}_3)$	1377	1377
--	--	1261	$\nu(\text{C-C})$, $\delta(\text{C-H})$	--	--
1238	$\nu_{\text{as}}(\text{C-O})$ in ester	1240	$\nu(\text{C-O})$	1238	1232sh
--	--	1179	$\delta(\text{C-H})$, $\nu(\text{C-O})$	--	1175
1164	$\nu_{\text{as}}(\text{C-C-O})$ in ester	1150	--	1160sh-1150	--
1100	$\nu_{\text{as}}(\text{O-CH}_2\text{-C})$	1106	$\delta(\text{C-H})$, $\nu(\text{C-O})$	1100	1097
--	--	1084	$\delta(\text{C-H})$, $\nu(\text{C-O})$	1100	--
--	--	1030	$\delta(\text{C-H})$, $\nu(\text{C-O})$	1030	1030sh
--	--	889	ω, τ (CH_2) in vinylidene structure	889	--
723	$\gamma(\text{CH}_2)+ \omega, \tau$ (C-H) in CH=CH <i>cis</i>	--	--	723	--

^a ν : stretching; δ : bending; ω : wagging; τ : twisting; γ : rocking; as: asymmetric; s: symmetric

Kinetic study

The photo-oxidation kinetics of solvent and oil based varnishes in terms of the measured absorbance variations of the C-H, C=O and O-H stretching bands as function of ageing time are summarized in Fig. 13. The integrated absorbance collected at each ageing time have been normalized to the starting value (A_{t_n}/A_{t_0}), thus making data independent from the thickness of the film of each varnish.

The plots show a similar decrease of the CH bands and increase of the C=O and O-H bands, thus evidencing similar alteration phenomena for all the present natural varnishes. At the same time, significant quantitative differences between their decay and rise behaviors can be observed. The degradation pathways of the two different categories of varnishes are discussed hereafter.

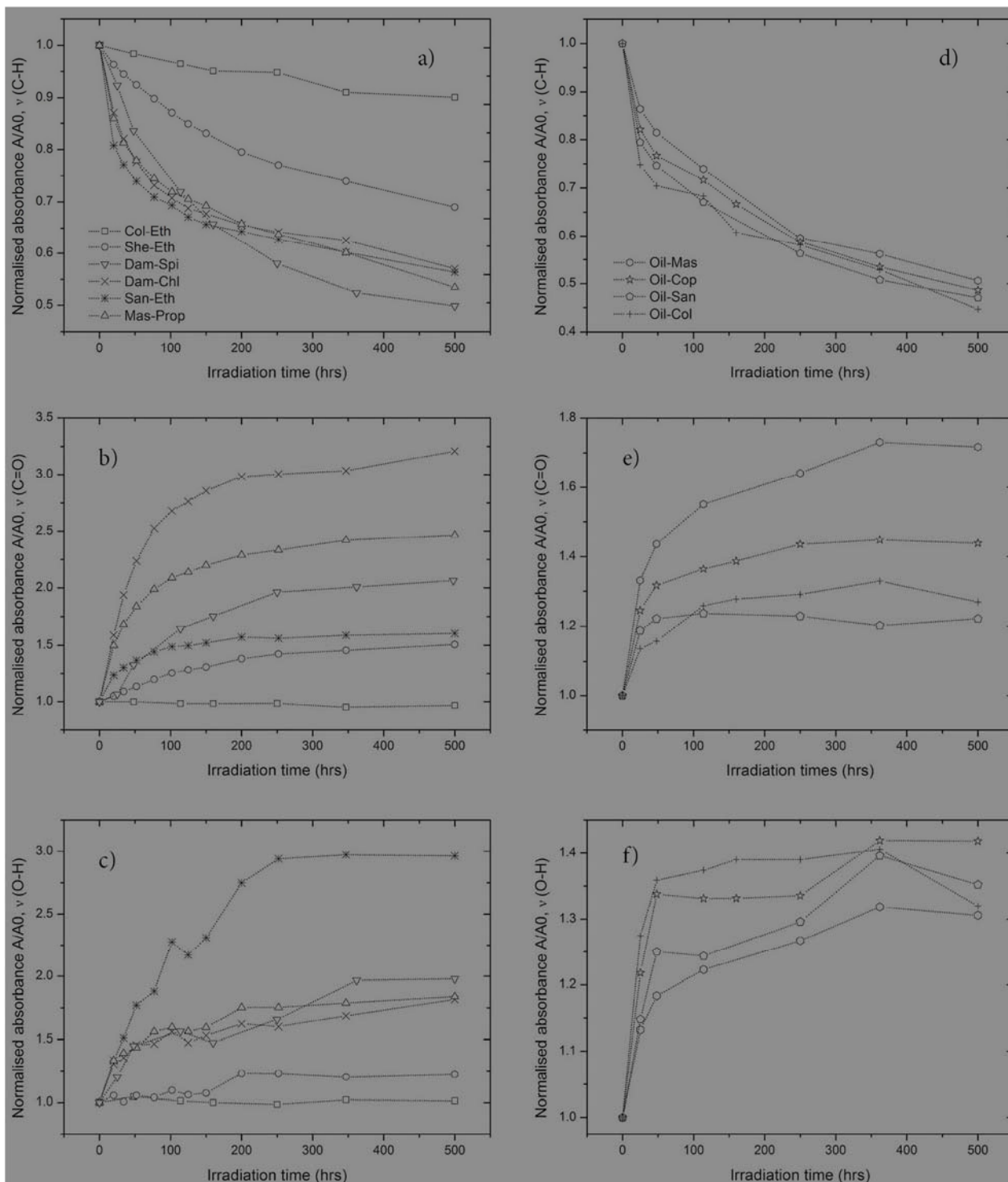


Fig. 13 Time evolution of C-H, C=O and O-H stretching bands for solvent (left) and oil (right) based varnishes during the aging.

Solvent varnishes

As shown in Fig.13a, the signal of C-H groups of Mas-Prop San-Eth Dam-Chl and Dam-Spi underwent an exponential decay during aging. The decrease of absorbance ratios was about 25% within the first 50 h of ageing to reach 50% after 500 h. She-Eth and much less Col-Eth, did not follow the same fast decay. These trends suggest that kinetics of photo-oxidation reactions, which start with hydrogen abstraction from methyl and methylene functional groups, depend on the

molecular structure of the specific terpenoid compounds although this does not exactly reflect their classification.

As reported in literature [15,17,20,21,40, 43], oxidation of triterpenoids undergoes A-ring opening through Norrish I type reactions upon irradiation under intense light fluxes. The resultant A-ring cleavage to a diradical (Norrish type I reaction) can be followed by oxygen insertion leading to carboxylates, aldehydes, peroxides, hydroperoxides and lactones. The latter are the main components of oxidized dammarane skeleton type molecules, as found to occur in naturally aged paintings. All these reactions are in agreement with the increase and broadening observed in the signal of C=O and OH groups (Fig. 13b-c), as well as in the 900-1300 cm^{-1} region due to C-O stretching absorption.

However, oxidation of di- and triterpene double bonds and hydroxylation of triterpene keto group cannot provide a plausible explanation of the slight increase of the b^* colorimetric coordinates, which indicate the beginning of a yellowing effect. This means that other degradation reactions take place concurrently. Thus, intramolecular termination reactions lead to unsaturated ketones, such as quinones, to which yellowing of natural resins is ascribable [14-15-40]. It was demonstrated that these high molecular weight fractions are cross-linked in the outer varnish layer, precisely in the first 10 micron [21]. Nevertheless, the increase in b^* coordinate was not so intense to be appreciated to naked eye, thus indicating a very low amount of yellow chromophores. In fact, yellowing is mainly observed to develop in darkness and not under accelerated light exposure, in which bleaching preferably occurs due to strong autoxidation [14,16]. However, FTIR did not detect the presence of such compounds, probably due to their low concentration (below the detection limit).

Diterpenoid varnishes, such as San-Eth and Col-Eth, do not follow the same photo-oxidation kinetics (Fig. 13a). The peaks of C-H groups in San-Eth decrease exponentially, as previously observed for triterpenoids varnishes, while in Col-Eth the change was almost negligible. It is worth noting that the carbonyl absorption in both the diterpenoid resins decreases and broadens, which is exactly opposite to that of triterpenoid resins. This feature is clearly distinguishable by observing the spectral intensities (Fig. 14). It can be attributed to a major ability of diterpenoids to undergo polymerization in place of oxidation, with respect to triterpenoids. Besides this, hydroxylation was stronger in San-Eth than Col-Eth, which suggests that the polymerization increases the acidity of the aged film. The same trend has been evidenced also in the C-O stretching region. Sandarac, being mainly constituted of pimarane and labdane compounds, is readily prone to polymerization due to the presence of a vinyl group on the side chain. In fact, as shown by FTIR data, San-Eth polymerises rapidly at two C=C sites through the loss of unsaturations belonging to *trans*-communic acid fraction. The other minor amount of pimaranes molecules of sandarac, such as agathic and sandaracopimaric acids, do not provide a substantial contribution to cross-linking due to the lack of conjugated double bonds [18-19-29]. Contrarily, reactive conjugated double bonds are also present in abietane-type molecules of colophony but mostly inside the C-ring (weak IR signal), which result reasonably less susceptible to breakdown [17]. This suggests the cross-linking reactions were not the same as those of communic acid-based polymers where the reactive C=C are in the side chain. For this reason, colophony easily undergoes dehydrogenation and aromatization processes during ageing leading to a conversion of abietic and neoabietic acid into dehydroabietic acid, which is present in fresh material as 5-10%. The FTIR signals at 1611 and 1495 cm^{-1} slightly increase during ageing, thus confirming an increase in aromatic structures; the dehydrogenated compounds are coloured chromophores characterized by a less photosensitive structure, due to the presence of an aromatic ring.

These compositional differences suggest that pimarane and labdane compounds are more susceptible than abietanes to photo-oxidation reactions, as evidenced also by quasi-linear ageing kinetic of the Col-Eth. Remarkable differences were detected also from the colourimetric standpoint. As described, the increase of b^* coordinate for sandarac was below the detection limit of human eye, whereas for colophony a strong darkening toward brown-orange hue could be well appreciated also to naked eye after only 20 h light exposure. The strong colour variation, which is fully in agreement with what reported in literature about pine resins, could confirm the formation of dehydroabietic acid [41-42]. In particular, pine colophony, has the notoriously bad reputation of darkening and becoming brittle over time [18].

Finally, the spectral features of bleached shellac upon photo-induced ageing suggest clearly that the cross-linking process is driven by self-esterification (increase of bands at 1735 and 1171 cm^{-1}) and looks similar to unbleached one [3, 23, 30-31]. The starting point of such a process can be related to the dissociation of aldehyde and carboxylic acid functions, as shown by the kinetic study. Surprisingly, the colourimetric measurements have shown that, contrarily to the other terpenoid resins studied, bleached shellac undergoes further bleaching upon irradiation, which was also appreciable to the naked eye. This effect can be related to a certain amount of chlorine residue, which acts as a bleaching agent in the varnish through the absorption of the blue light component (around 400 nm) [44]. Most likely, a transfer of energy from chlorine to neighboring molecules starts a chain of chemical events which can be seen as post irradiation effect.

Additional information may be obtained by plotting the peak height ratio of the C=O (Fig. 14).

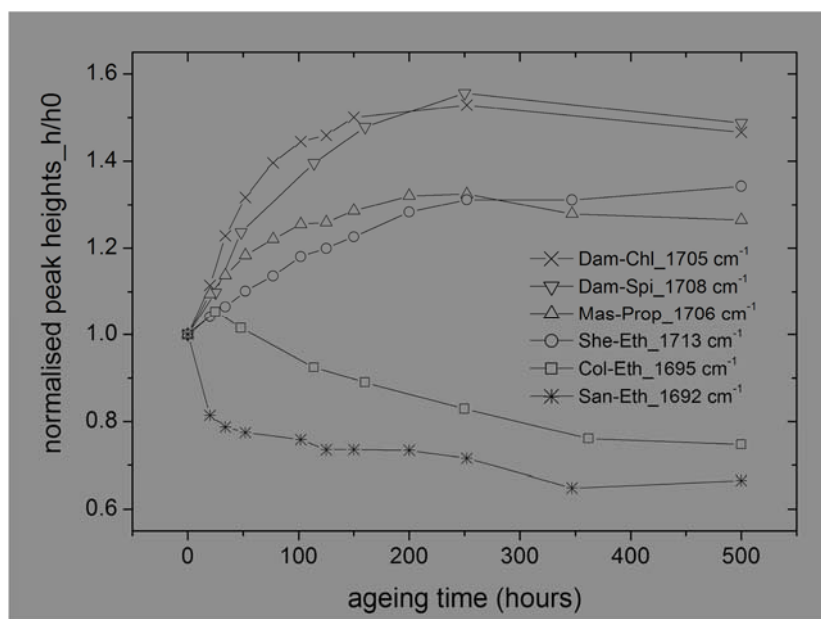


Fig. 14 Peak height ratio of the C=O stretching bands of solvent varnishes as function of the ageing time

The behaviors of Fig. 14 along with those of $\nu(\text{C}=\text{O})$ reported in Fig. 13b confirm the opposite trends of Col-Eth and San-Eth with respect to Dam-Spi, Mas-Prop and She-Eth. Such a different light interaction result arises from the different structure of the terpenoid compounds under study. The low wavenumber of the carbonyl stretching bands in Col-Eth and San-Eth (1695 and 1693 cm^{-1} , respectively) is attributed to the presence of carboxylic acids with internal/intermolecular hydrogen bonding, which condensation reactions lead to new carbonyl structures (i.e. esters, anhydrides, lactones). On the contrary, the higher wavenumber in Dam-Spi, Mas-Prop, and She-

Eth (1705, 1706 and 1713 cm^{-1}) due to a lower degree of inter/intramolecular hydrogen bonding decreases the possibility of condensation.

This means that the height of the C=O stretching of acids in Col-Eth and San-Eth is reduced after irradiation, but not in the case of Dam-Spi, Mas-Pro and She-Eth. At the same time, for Col-Eth and San-Eth an increase of the C=O stretching signal intensity of condensed compounds is expected. Actually, in the case of Col-Eth, the peak decreased but the area of the C=O remained constant. In the case of San-Eth the decrease of the peak was compensated by modest increase in the integral.

Taking into account the presence of reactive C=C double bonds (i.e. in communic acid), the oxidation of these groups is competitive with the condensation of carboxylic acids and a general increase of the area of the total C=O groups was expected and found.

In the case of Dam-Spi and Mas-Prop, the simultaneous increase of the peak heights and area can be attributed to the prevalence of oxidation (reactive double bonds) with the formation of new carboxylic acids and other oxidized carbonyl structures (i.e. esters, anhydrides, lactones). Finally, the She-Eth did not show so much reactive groups because less new carboxylic acids and carbonyl compounds than in Mas-Prop and Dam-Spi were formed.

Oil varnishes

Oil varnishes showed noticeable differences after the heat processing at relatively high temperatures (220-285 $^{\circ}\text{C}$). First of all, the end-product resulted in an advanced oxidation, condensed and very viscous state due to both the evaporation of the volatile fraction from the boiling mixture and the presence of cobalt driers [24]. At the molecular level, the most relevant changes resulting from the thermal treatment involved the increase of acidic functional groups (OH, CO and COO stretching signals) and *cis-trans* isomerization of the double bonds in fatty acids (decreasing or complete disappearance of *cis* bands at 3010 and 722 cm^{-1} , appearance of *trans* conjugated and *trans* non-conjugated bands at 985 cm^{-1}). As reported in the literature [32], oleic acid, as a monounsaturated acid, can be oxidized only at high temperatures, while polyunsaturated acids such as linolenic and linoleic acids undergo rapid oxidation even at room temperature. In addition, in presence of cobalt driers the cross-linking took place very quickly (200 min) and the kinetic was faster than pure linseed oil (240 h) [24-33]. Surely, several products formed via thermal breakdown of acyl chains on both sides of double bonds (i.e. alkanes, alkenes and short chains of unsaturated fatty acids), were not detected by FTIR.

Despite some changes were noticed, after a curing period of one month, in free oxygen conditions the infrared bands of the resin and oil were still appreciable. On the opposite, after only 20 h of light exposure both the components were hardly recognizable due to the loss of representative spectral features. The first important chemical reaction taking place during the initial drying of an oil varnish comes as a result of an intense oxygen-mediated process, as demonstrated also by the weight rises. The content of carbonyl, hydroxyl and hydroperoxydes increased and broadened notably. Simultaneously, the kinetics of CH groups including stretching and bending modes shows also that such process does not depend on the type of terpenoid resin in the mixture. This is governed by the oil *via* hydrogen abstraction on a methylene group between two double bonds in polyunsaturated fatty acid chain. As known, this is the first step of an oxidation process leading to conjugated and/or non-conjugated hydroperoxydes (ROOH). After decomposition of the latter, oxygenated structures, such as alcohols, aldehydes, ketones and different carbonyl groups or cross-linking products are formed as well as low molecular weight compounds, which can evaporate or

remain linked to glyceride molecules without taking part to cross-linking [14, 33, 34,36]. Basically, the linseed oil content in the varnish, owing to the presence of many unsaturations, gives a significant contribution to oxidation through the formation of hydroperoxides. On the other hand, the compounds with the higher degree of unsaturation after heat processing and light exposure oxidize and polymerize faster thus making limited their spectral detection.

Conclusions

In this work, the photo-induced oxidation effects of different types of solvent and oil terpenoid-based varnishes, usually encountered in conservation of easel paintings, were characterized using FTIR transmission spectroscopy along with colorimetric and gravimetric measurements. It was found that the light-induced alterations, in di- (i.e. sandarac, colophony, Manila copal) tri- (i.e. mastic and dammar) and sesquiterpenic (i.e. bleached shellac) resins, either with or without a drying oil, typically begin with a hydrogen abstraction. The latter does not depend on the resin type when polyunsaturated fatty acids are present in the varnish. Thereafter, the action of oxygen-mediated processes catalyzed by intense radiation and temperature rise lead to the formation of new carboxylic acids and to the condensation of the existing acidic compounds in other oxidized carbonyl structures (i.e. esters, anhydrides, lactones). In triterpenoid resins and much less in shellac, both these reactions take place concurrently while in diterpenoids condensation is more efficient (i.e. sandarac and copal), except for colophony which undergoes mainly aromatization.

Cross-linking, extensive polymerization and degradation phenomena occur, in different extent, depending on the type of unsaturation of the material. Thus for instance, the cross-linking reactions, which are prominent in sandarac, copal and shellac resins due to the cleavage of C=C (loss of unsaturations), may be easily monitored by FTIR spectroscopy. Such reactions explain the slight weight loss observed, which are associated with the loss of volatile compounds, such as monoterpenes and low molecular weight terpenic degradation products. No significant yellowing was evidenced for dammar, mastic and sandarac. Colophony underwent a noticeable darkening after only 20h of ageing, most likely due to the formation of coloured polycyclic aromatic structures. On the contrary, bleached shellac showed further bleaching during ageing most likely due to the residual chlorine.

The C-H stretching and bending modes along with C-O stretching represent the most meaningful peaks for assessing the light-induced changes. In particular, the $\nu(\text{C-H})/\nu(\text{C-O})$ may be considered as a suitable indicator of the photo-oxidative degradation in natural varnishes.

Finally, besides the interpretation of the different deterioration pathways of the varnishes investigated, this study also provides information on their relative stability, which should be taken into account in conservation of artworks. Thus in particular, we have shown that bleached shellac, exhibits the highest resistance to the photo-oxidation since light exposure mainly produces polymerization. This feature along with the high transparency and low cracking of the mentioned resin could make it the best natural varnish, but its pronounced cross-linking produces serious reversibility problems. Anyway, if the future developments of the nanostructured detergents and of the laser ablation techniques will suitably address such an issue, bleached shellac could get a widespread finishing coating.

Further insights will be devoted to the present topic in order to improve the identification of specific compounds produced during light-ageing.

Acknowledgments The present work was supported by the PEGASO project (POR FSE 2007-2013) funded by Tuscany Region.

References

- [1] E.R. de la Rie, The influence of varnishes on the appearance of paintings, *Stud. Conserv.* 32 (1987) 1–13. doi:10.2307/1506186.
- [2] E.R. De La Rie, Old master paintings: a study of the varnish problem, *Anal. Chem.* 61 (1989) 1228A–1237A. doi:10.1021/ac00196a003.
- [3] J. S. Mills, R. White, *The Organic Chemistry of Museum Objects*. Routledge, 1999.
- [4] M. Elias, E. René de la Rie, J.K. Delaney, E. Charron, K.M. Morales, Modification of the surface state of rough substrates by two different varnishes and influence on the reflected light, *Opt. Commun.* 266 (2006) 586–591. doi:10.1016/j.optcom.2006.05.051.
- [5] K. Sutherland, Solvent-extractable components of linseed oil paint films, *Stud. Conserv.* 48 (2003) 111–135. doi:10.2307/1506796.
- [6] De Mayerne, T. T.. *Pictoria, Sculptoria, Tinctoria, et quae subalternarum artium*. Manuscript (British Museum London, Ms. Sloane 2052, 1901:1620-1642.
- [7] Dodwell CR, editor. *Theophilus, De Diversis Artibus*, Oxford, 1961.
- [8] Watin, J. F. *L'Art du peintre, doreur, vernisseur, ouvrage utile aux artistes et aux amateurs*. Grangé, 1773.
- [9] Merrifield M.P. *Original Treatises on the arts of Painting*, London, 1849.
- [10] Eastlake, S. C. L. *Methods and materials of painting of the great schools and masters (Vol. 1)*. Dover Publications: 1960.
- [11] J. Mills, R. White, Natural resins of art and archaeology their sources, chemistry, and identification, *Stud. Conserv.* 22 (1977) 12–31. doi:10.2307/1505670.
- [12] P. Dietemann, C. Higgitt, M. Kälin, M.J. Edelmann, R. Knochenmuss, R. Zenobi, Aging and yellowing of triterpenoid resin varnishes - Influence of aging conditions and resin composition, *J. Cult. Herit.* 10 (2009) 30–40. doi:10.1016/j.culher.2008.04.007.
- [13] N. S. Allen, M. Edge. *Fundamentals of polymer degradation and stabilization*. Springer Netherlands, 1993.
- [14] E.R. de la Rie, Photochemical and thermal degradation of films of dammar resin, *Stud. Conserv.* 33 (1988) 53–70.
- [15] G.A. van der Doelen, *Molecular studies of fresh and aged triterpenoid varnishes*, 1999.
- [16] R. L. Feller. *Accelerated aging: photochemical and thermal aspects*. Getty Publications, 1995.
- [17] C. Theodorakopoulos. *The Excimer Laser Ablation of Picture Varnishes: An evaluation with reference to light-induced deterioration*, PhD thesis, Royal College of Art, RCA/V&A Conservation, London, 2005.
- [18] D. Scalarone, M. Lazzari, O. Chiantore, Ageing behaviour and analytical pyrolysis characterisation of diterpenic resins used as art materials: Manila copal and sandarac, *J. Anal. Appl. Pyrolysis.* 68-69 (2003) 115–136. doi:10.1016/S0165-2370(03)00005-6.
- [19] D. Scalarone, M. Lazzari, O. Chiantore, Ageing behavior and pyrolytic characterization of diterpenic resins used as art materials: colophony and Venice turpentine, *J. Anal. Appl. Pyrolysis.* 64 (2002) 345–361. doi:10.1016/S0165-2370(02)00046-3.

- [20] S. Zumbühl, R. Knochenmuss, S. Wülfert, F. Dubois, M. J. Dale, R. Zenobi. A graphite-assisted laser desorption/ionization study of light-induced aging in triterpene dammar and mastic varnishes. *Anal Chem* 70 (1998) 707-715. doi: 10.1021/ac970574.
- [21] C. Theodorakopoulos, V. Zafirooulos, J.J. Boon, S.C. Boyatzis, Spectroscopic investigations on the depth-dependent degradation gradients of aged triterpenoid varnishes, *Appl. Spectrosc.* 61 (2007) 1045–1051. doi:10.1366/000370207782217833.
- [22] S. Limmatvapirat, C. Limmatvapirat, S. Puttipipatkachorn, J. Nuntanid, M. Luangtananan. Enhanced enteric properties and stability of shellac films through composite salts formation. *Eur J Pharm Biopharm*, 67 (2007) 690-698. doi:10.1016/j.ejpb.2007.04.008
- [23] Y. Farag, Characterization of Different Shellac Types and Development of Shellac-Coated Dosage Forms, (2010) 143.
- [24] J. Mallécol, J. Lemaire, J.L. Gardette, Drier influence on the curing of linseed oil, *Prog. Org. Coatings*. 39 (2000) 107–113. doi:10.1016/S0300-9440(00)00126-0.
- [25] M. R. Derrick, D. Stulik, J. M. Landry. *Infrared spectroscopy in conservation science*. Getty Publications, 2000.
- [26] M. Hesse, H. Meier, B. Zeeh. *Spectroscopic methods in organic chemistry*. Stuttgart: Thieme. 2008.
- [27] G. L. Shearer. An evaluation of Fourier transform infrared spectroscopy for the characterization of organic compounds in art and archaeology, PhD thesis, University of London, 1989.
- [28] C. Azémard, C. Vieillescazes, M. Ménager, Effect of photodegradation on the identification of natural varnishes by FT-IR spectroscopy, *Microchem. J.* 112 (2014) 137–149. doi:10.1016/j.microc.2013.09.020.
- [29] M. Villanueva-García, A. Martínez-Richa, J. Robles. Assignment of vibrational spectra of labdatriene derivatives and ambers: a combined experimental and density functional theoretical study. *Arkivoc* 6 (2005) 449-458. <http://dx.doi.org/10.3998/ark.5550190.0006.639>
- [30] C. Coelho, R. Nanabala, M. Ménager, S. Commereuc, V. Verney, Molecular changes during natural biopolymer ageing - The case of shellac, *Polym. Degrad. Stab.* 97 (2012) 936–940. doi:10.1016/j.polymdegradstab.2012.03.024.
- [31] J. Derry. *Investigating Shellac: Documenting the Process, Defining the Product: A study on the processing methods of Shellac, and the analysis of selected physical and chemical characteristics*, Master thesis, University of Oslo, 2012.
- [32] B. Dlugogorski, E. Kennedy, J. Mackie, Low temperature oxidation of linseed oil: a review, *Fire Sci. Rev.* (2012) 1–36. doi:10.1186/2193-0414-1-3.
- [33] J.D.J. van den Berg, N.D. Vermist, L. Carlyle, M. Holcapek, J.J. Boon, Effects of traditional processing methods of linseed oil on the composition of its triacylglycerols., *J. Sep. Sci.* 27 (2004) 181–199. doi:10.1002/jssc.200301610.
- [34] M. Lazzari, O. Chiantore, Drying and oxidative degradation of linseed oil, *Polym. Degrad. Stab.* 65 (1999) 303–313. doi:10.1016/S0141-3910(99)00020-8.
- [35] J. Mallécol, J.-L. Gardette, J. Lemaire, Long-term behavior of oil-based varnishes and paints I. Spectroscopic analysis of curing drying oils, *J. Am. Oil Chem. Soc.* 76 (1999) 967–976. doi:10.1007/s11746-999-0114-3.
- [36] R. J. Meilunas, J. G. Bentsen, A. Steinberg. Analysis of aged paint binders by FTIR spectroscopy. *Stud Conserv* 35 (1990) 33-51. doi: 10.1179/sic.1990.35.1.33

- [37] J. Mallécol, J.-L. Gardette, J. Lemaire, Long-term behavior of oil-based varnishes and paints. Photo- and thermooxidation of cured linseed oil, *J. Am. Oil Chem. Soc.* 77 (2000) 257–263. doi:10.1007/s11746-000-0042-4.
- [38] N. Marchand-Geneste, a. Carpy, Theoretical study of the thermal degradation pathways of abietane skeleton diterpenoids: Aromatization to retene, *J. Mol. Struct. THEOCHEM.* 635 (2003) 55–82. doi:10.1016/S0166-1280(03)00401-9.
- [39] R. M. Carman, D. E. Cowley, R. A. Marty, Diterpenoids. XXV. Dundathic acid and polycommunic acid. *Aust. J. Chem* 23 (1970) 1655-1665. doi:10.1071/CH9701655
- [40] P. Dietemann, Towards More Stable Natural Resin Varnishes for Paintings - The Aging of Triterpenoid Resins and Varnishes, (2003) 1–196. doi:10.3929/ethz-a-004621911.
- [41] K. J. Van den Berg, Analysis of Diterpenoid Resins and Polymers in Paint Media and Varnishes: With an Atlas of Mass Spectra. FOM Institute AMOLF 2012
- [42] A. Findeisen, V. Kolivoska, I. Kaml, W. Baatz, E. Kenndler, Analysis of diterpenoic compounds in natural resins applied as binders in museum objects by capillary electrophoresis., *J. Chromatogr. A.* 1157 (2007) 454–61. doi:10.1016/j.chroma.2007.05.010.
- [43] A. Nevin, D. Comelli, I. Osticioli, L. Toniolo, G. Valentini, R. Cubeddu, Assessment of the ageing of triterpenoid paint varnishes using fluorescence, Raman and FTIR spectroscopy, *Anal. Bioanal. Chem.* 395 (2009) 2139–2149. doi:10.1007/s00216-009-3005-4.
- [44] K. Sutherland, Bleached shellac picture varnishes: characterization and case studies, *J. Inst. Conserv.* 33 (2010) 129–145. doi:10.1080/19455224.2010.495242.